

# The yeast mitochondrial ADP/ATP carrier functions as a monomer in mitochondrial membranes

Lisa Bamber, Marilyn Harding, Magnus Monné\*, Dirk-Jan Slotboom†, and Edmund R. S. Kunji‡

Medical Research Council, Dunn Human Nutrition Unit, Hills Road, Cambridge CB2 2XY, United Kingdom

Communicated by John E. Walker, Medical Research Council, Cambridge, United Kingdom, April 30, 2007 (received for review March 29, 2007)

Mitochondrial carriers are believed widely to be dimers both in structure and function. However, the structural fold is a barrel of six transmembrane  $\alpha$ -helices without an obvious dimerisation interface. Here, we show by negative dominance studies that the yeast mitochondrial ADP/ATP carrier 2 from *Saccharomyces cerevisiae* (AAC2) is functional as a monomer in the mitochondrial membrane. Adenine nucleotide transport by wild-type AAC2 is inhibited by the sulfhydryl reagent 2-sulfonatoethyl-methanethiosulfonate (MTSES), whereas the activity of a mutant AAC2, devoid of cysteines, is unaffected. Wild-type and cysteine-less AAC2 were coexpressed in different molar ratios in yeast mitochondrial membranes. After addition of MTSES the residual transport activity correlated linearly with the fraction of cysteine-less carrier present in the membranes, and so the two versions functioned independently of each other. Also, the cysteine-less and wild-type carriers were purified separately, mixed in defined ratios and reconstituted into liposomes. Again, the residual transport activity in the presence of MTSES depended linearly on the amount of cysteine-less carrier. Thus, the entire transport cycle for ADP/ATP exchange is carried out by the monomer.

mechanism | membrane protein | negative dominance studies | oligomeric state | transport

Mitochondrial carriers are believed widely to exist and function as homo-dimers (1–23). However, structural data are inconsistent with biochemical and biophysical studies that have been used to provide support for the existence of dimers in membranes and in detergents. First, the projection structure of the mitochondrial yeast ADP/ATP carrier demonstrated that the structural fold consists of six transmembrane (TM)  $\alpha$ -helices rather than an intercalated bundle of twelve  $\alpha$ -helices (24). Second, there are no extensive protein-protein interfaces between neighboring carriers in the crystals, as would be expected for proteins that require cooperative interaction to function (25). Third, the density distribution had 3-fold pseudo symmetry in agreement with the 3-fold sequence repeats found in all mitochondrial carriers (26, 27). Fourth, the substrate translocation pathway appeared to be in the centre of the protein, rather than at the interface between two monomers (24). Fifth, although the proteins formed two-dimensional crystals of dimers in rows in both the  $P22_12_1$  and  $P2$  crystal forms (24), it was monomeric in detergent before crystal formation (28). Sixth, the atomic structure of the bovine ADP/ATP carrier in detergent determined by x-ray crystallography of  $P2_12_12$  and  $C222_1$  crystal forms showed that the structural fold was a six- $\alpha$ -helical bundle with three additional short  $\alpha$ -helices in the mitochondrial matrix (13). Seventh, the  $P2_12_12$  crystal did not contain pairs of interacting proteins with the same orientation (13), but the  $C222_1$  crystal contained two types of dimers, one of which has been proposed to be biologically significant (11, 29). However, all of the protein-protein interactions in these crystals are mediated by proteins with different orientations, and so the dimers probably have been formed during crystallization. Eighth, the pseudo 3-fold axis of symmetry in the  $C222_1$  crystal is at  $\approx 10^\circ$  to the plane of the membrane, which is incompatible with sequence and structural conservation of symmetry, and the density distribution in the projection structure of AAC3 (24). Ninth, homo-dimer

formation in the  $C222_1$  crystal is mediated entirely by cardiolipins (11), and it is difficult to see how this type of interaction could provide a means for cooperativity and for the formation of specific homo-dimers in the presence many structurally related but functionally different carriers in mitochondrial membranes. Tenth, as with the  $P22_12_1$  and  $P2$  crystals (24), both monomers of the dimer bind atractylosides and so they are in the same rather than in the opposed state. Finally, the dimer interface in the  $P22_12_1$  crystals (24) differs from that in the  $C222_1$  crystal (11), and so there is no consistent interaction interface. Thus, there is no structural explanation of how the dimers might form. Recently, we have shown that the yeast ADP/ATP carrier is monomeric in a wide range of detergents (28), but the question of whether the monomers are associated into homo-dimers in the membrane has remained unresolved.

Here, we have investigated by negative dominance studies whether a yeast ADP/ATP carrier in the mitochondrial membrane needs to be associated to function. This approach is based on dimers becoming dysfunctional when one protomer is disabled. It has been used to show that lactose permease LacY functions as a monomer (30), that the small drug transporter EmrE functions as an oligomer (31), and that maltoporin functions as a trimer with three distinct selectivity filters (32, 33). To establish the functional interaction between monomers, it must be possible to inactivate one protomer and to leave the second monomer unmodified and active. The yeast ADP/ATP carrier can be inactivated by sulfhydryl reagents, but replacement of its four cysteine residues by alanine provides a fully active carrier (34). Wild-type and cysteine-less ADP/ATP carriers were coexpressed in various molar ratios in mitochondrial membranes. The function of the cysteine-less ADP/ATP carrier 2 from *Saccharomyces cerevisiae* (AAC2) was unaffected by the inhibition of the coexpressed wild-type carriers, and so the two forms function independently. In addition, the cysteine-less and wild-type carriers were purified, mixed in defined ratios and reconstituted into liposomes. After addition of the sulfhydryl reagent, the residual transport rate correlated linearly with the fraction of cysteine-less AAC2, indicating that there is no functional association between AAC2 protomers. Thus, the yeast mitochondrial ADP/ATP carriers function as monomers in membranes.

Author contributions: D.-J.S. and E.R.S.K. designed research; L.B., M.H., M.M., D.-J.S., and E.R.S.K. performed research; L.B., M.H., M.M., and E.R.S.K. analyzed data; and E.R.S.K. wrote the paper.

The authors declare no conflict of interest.

Freely available online through the PNAS open access option.

Abbreviations: ATR, atractyloside; AAC2, ADP/ATP carrier 2 from *S. cerevisiae*; MTSES, 2-sulfonatoethyl-methanethiosulfonate; KPI, potassium phosphate buffer; TM, transmembrane.

\*Present address: Department of Biosciences and Nutrition, Karolinska Institute, Hålsövägen 7-9, 141 57 Huddinge, Stockholm, Sweden.

†Present address: Department of Biochemistry, University of Groningen, Nijenborg 4, 9747 AG Groningen, The Netherlands.

‡To whom correspondence should be addressed. E-mail: ek@mrc-dunn.cam.ac.uk.

This article contains supporting information online at [www.pnas.org/cgi/content/full/0703969104/DC1](http://www.pnas.org/cgi/content/full/0703969104/DC1).

© 2007 by The National Academy of Sciences of the USA



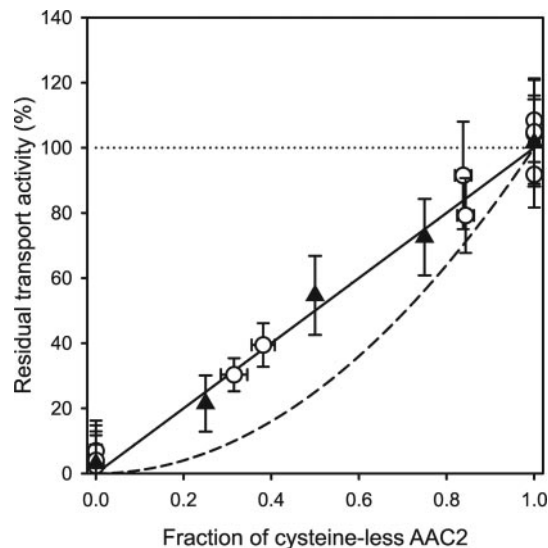


**Fig. 3.** Correlation between the fraction of cysteine-less AAC2 and the residual initial transport rate after addition of MTSES. The residual initial transport rate in the presence of MTSES is expressed as a percentage of the rate in the absence of MTSES. Open circles represent the residual rate of coexpressed wild-type and/or cysteine-less AAC2 in mitochondrial membranes. The average rate in the absence of MTSES (100%, dotted line) was  $20.6 \pm 2.7$  nmol·min<sup>-1</sup>·mg<sup>-1</sup> of AAC2 (raw data from Fig. 2). The closed triangles indicate the residual transport rate of wild-type and/or cysteine-less AAC2, purified separately and mixed in defined molar ratios and then reconstituted into liposomes. In this case, the average rate was  $16.4 \pm 4.6$  nmol·min<sup>-1</sup>·mg<sup>-1</sup> of AAC2 in the absence of MTSES (100%, dotted line). The initial uptake rates of [<sup>14</sup>C]-ADP were determined in quintuplicate in the first 15 s of linear uptake. The amount of AAC2 in the fused mitochondrial membranes or proteoliposomes was quantified in triplicate by using Western blot analyses and known amounts of purified AAC2 as standard. The continuous and dashed lines represent the theoretical correlation for the independent and dependent functional interactions of the cysteine-less AAC2 and wild-type AAC2, respectively.

(average of  $20.6 \pm 2.7$  nmol min<sup>-1</sup> mg<sup>-1</sup> of AAC2) for all version of AAC2 whether they were expressed as single or as tandem combinations (Fig. 2C). The average specific initial uptake rate for the cysteine-less carrier was similar to that of the wild-type AAC2 ( $20.2 \pm 1.2$  versus  $20.9 \pm 1.2$  nmol·min<sup>-1</sup>·mg<sup>-1</sup> of AAC2), confirming that the alanine substitutions did not affect the function of the carrier (Fig. 2C). The introduction of a six-histidine tag had no effect on function either, because the average values in the absence of MTSES were  $20.6 \pm 1.0$  and  $20.4 \pm 1.5$  nmol·min<sup>-1</sup>·mg<sup>-1</sup> of AAC2 for untagged and tagged AAC2, respectively. Wild-type AAC2 was inhibited fully by the addition of MTSES, whereas cysteine-less AAC2 was unaffected (Fig. 2C). The specific initial uptake transport rates of the coexpressed *Ppic2-XCL+Ppic2-HWT* and *Paac2-XCL+Paac2-HWT* were reduced by the addition of MTSES to 90 and 78%, respectively. The addition of MTSES affected coexpressed *Paac2-XWT+Paac2-HCL* and *Ppic2-XWT+Ppic2-HCL* to a greater extent, leading to a reduction of transport rate to 39 and 30%, respectively. The residual transport activity correlated linearly with the fraction of cysteine-less AAC2 present in the membrane (Fig. 3). Therefore, the cysteine-less and wild-type carriers functioned independently.

**Reconstitution of Cysteine-Less and Wild-Type AAC2 in Defined Molar Ratios.** The cysteine-less AAC2 and wild-type AAC2 in complex with ATR were purified separately in dodecylmaltoside, where AAC2 is monomeric (28), mixed in a defined ratio and reconstituted into liposomes. After reconstitution of the carriers into

liposomes, ATR was displaced with ADP. The specific initial rate of uptake of ADP in the absence of MTSES was  $16.4 \pm 4.6$  nmol·min<sup>-1</sup>·mg<sup>-1</sup> of AAC2, which is slightly lower than the value found for the carrier in mitochondrial membranes, and so the reconstitution procedure was efficient. The slightly lower value may be due to the loss of small amounts of functional material during insertion, or to incomplete reversal of ATR inhibition or to the lipid environment, not mimicking the mitochondrial membrane. Again, the residual transport activity after addition of MTSES correlated linearly with the fraction of cysteine-less AAC2 that had been added to the mixture before reconstitution (Fig. 3).

## Discussion

Here, the possible association of the monomers of the yeast ADP/ATP carrier AAC2 to form functional dimers was tested by negative dominance studies. The approach exploits the sensitivity of the wild-type AAC2 to sulfhydryl reagents (35), and the finding that the four cysteines in the wild-type AAC2 can be replaced by alanine without affecting its activity. When the cysteine-less and wild-type carriers were coexpressed in mitochondrial membranes, or mixed in defined ratios before being reconstituted in liposomes, the residual transport rate after addition of MTSES depended on the fraction of cysteine-less carrier in the membrane in a linear way (Fig. 3). The residual transport rates in the presence of MTSES fitted a power function, according to  $V_{\text{with MTSES}} = a \times F_{\text{cl}}^b$ . The fitted values were 102% and 1.03 for *a* and *b*, respectively, confirming that the cysteine-less and wild-type AAC2 functioned independently. The root mean square deviation was calculated between the experimental data and the theoretical curves taking the data points in the presence of MTSES ( $0 < F_{\text{cl}} < 1$ ) (Fig. 3). The root mean square deviation is 2.8% for functionally independent carriers, which is within experimental error. In contrast, the root mean square deviation would have been 13.1% if they had functioned in a 1:1 dimer. Thus, the cysteine-less and wild-type AAC2 function independently. It might be argued that the results could be explained by homo-dimers of cysteine-less AAC2 or homo-dimers of wild-type AAC2 forming preferentially. For example, the presence of a His-tag could lead to the dimerisation of this version exclusively. However, this possibility was eliminated by the reconstitution experiments, in which both the cysteine-less AAC2 and wild-type AAC2 were His-tagged. In addition, if dimerisation by the His-tags occurred, it would have to have been stronger than dimerisation by a protein-protein interface, otherwise hetero-dimers of the two versions of AAC2 would have formed. However, then the specific transport rates would be expected to be low as dimerisation required for function would have been impaired (Fig. 2). Another possibility was that if cysteines were involved in dimer formation, the wild-type AAC2 might dimerize specifically to the exclusion of the cysteine-less AAC2. However, because cysteine-less carriers would be unable to dimerize, the specific uptake rate of the cysteine-less carriers would be low. Also, the overall transport rate of the coexpressed carriers would be negligible in the presence of MTSES, because the cysteine-less carriers would be unable to dimerize efficiently and the wild-type carriers would be inhibited. The simplest explanation of our data is that the yeast mitochondrial ADP/ATP carriers function as monomers rather than dimers. This conclusion is consistent with its structure (13, 24) and the dimensions and molecular mass of the ADP/ATP carrier in detergents (28).

Transporters of organic compounds vary considerably in size, oligomeric state, and the position of the translocation pathway. The TM domains of ABC transporters (10, but most commonly six TM  $\alpha$ -helices) form dimers with the substrate transport pathway at their interface (36–38). Members of the major facilitator superfamily (12 TM  $\alpha$ -helices) consist of two struc-

turally similar protein domains (each of six TM  $\alpha$ -helices) through which the substrate passes (39–42). The minimal functional unit for substrate binding in the multidrug transporter EmrE (four TM  $\alpha$ -helices) is also a dimer with the substrate binding at the monomer-monomer interface (43, 44). Aquaporins and glycerol transporters (six TM  $\alpha$ -helices plus two half-spanning  $\alpha$ -helices) are tetramers with a substrate translocation pore in each monomer (45–47). The glutamate transporter (eight TM  $\alpha$ -helices and two  $\alpha$ -helical hairpins) (48), the ammonium channel (11 TM  $\alpha$ -helices) (49), and the multidrug transporter AcrB (12 TM  $\alpha$ -helices) (50) are trimers, whereas the leucine and aspartate transporters (10 TM  $\alpha$ -helices plus two interrupted TM  $\alpha$ -helices) are dimers (51, 52), but each monomer contains a substrate binding site.

In mitochondrial carriers the substrate is translocated via a pathway in the middle of the structural fold of the protein, which is formed by six TM  $\alpha$ -helices (13, 24, 53, 54). Therefore, the ADP/ATP carrier is the smallest known functional transporter unit, and yet its substrates ADP and ATP are among the largest molecules that are actively transported across membranes. Other members of the mitochondrial carrier family transport even larger substrates like palmitoyl-carnitine (55, 56), CoA (57) or S-adenosyl-methionine (58). The transport of these substrates has to be achieved without any significant proton leak that would uncouple ATP synthesis from the proton motive force. These properties may explain why the mitochondrial ADP/ATP carrier transports substrates at a relatively low rate compared with members of other transporters families (59). Further studies into the structural mechanism of the mitochondrial carriers are required to understand how they accomplish this remarkable feat.

## Methods

**Construction of Expression Vectors.** A gene for the cysteine-less AAC2 was constructed by replacing all cysteine codons in wild-type *aac2* by alanine codons by using PCR overlap extension with KOD polymerase (Novagen, Madison, WI and EMD Biosciences, San Diego, CA). Vectors for the expression of the His-tagged and untagged versions of the wild-type and cysteine-less AAC2 as single proteins were based on the pYES-Ppic2-*aac2* and pYES-Ppic2-*His-aac2* vectors (28) or the pYES-Paac2-*His-aac2* and pYES-Paac2-*aac2* vectors (60). To obtain vectors for coexpression, the *aac2* gene (wild-type or cysteine-less), preceded by the *aac2* or *pic2* promoter region and followed by a transcription terminator, were introduced into the SpeI site at the start of the promoter region in the pYES-Ppic2-*His-aac2* vector or pYES-Paac2-*His-aac2* vector, containing the second type of *aac2*. SpeI sites were introduced by PCR with KOD polymerase (Novagen) at both ends of the promoter-*aac2*-transcription terminator cassette. Vectors and inserts were digested with SpeI (New England BioLabs, Ipswich, MA). The insert was ligated into the vector, and the vector was transformed into *Escherichia coli*. Because the insert could be inserted in both orientations, the desired version was identified by colony PCR and sequencing (Geneservice, Cambridge, U.K.). The vector containing the tandem expression cassette encoding wild-type and cysteine-less AAC2 was transformed into the *S. cerevisiae* strain WB-12 (MAT $\alpha$  *ade2-1 trp1-1 ura3-1 can1-100 aac1::LEU2 aac2::HIS3*), lacking functional AAC1 and AAC2 carriers (21).

**Preparation of Fused Mitochondrial Membranes for Transport Assays.** Yeast strains were grown as described in *SI Methods* and mitochondrial membranes were prepared as described in ref. 60. Liposomes were prepared with *E. coli* total lipid extract and egg yolk phosphatidylcholine (Avanti Polar Lipids, Alabaster, IL) mixed in a 3:1 (wt/wt) ratio in 50 mM potassium phosphate buffer (KPi), pH 7.0, at a final lipid concentration of 20 mg·ml<sup>-1</sup>.

Liposomes (5 mg·ml<sup>-1</sup>) and mitochondrial membranes (1 mg of protein ml<sup>-1</sup>) were fused by mixing in 50 mM KPi, pH 7.0, containing 5 mM ADP, followed by freezing in liquid nitrogen and thawing at room temperature 7 times.

**Inhibition and Purification of Yeast AAC2.** Mitochondrial membranes containing either wild-type or cysteine-less AAC2 were diluted to 20 mg·ml<sup>-1</sup> with buffer, consisting of 0.65 M sorbitol and 0.02 M Tris·HCl, pH 7.4. The membranes were incubated for 20 min at 4°C with ATR (Calbiochem, San Diego, CA and EMD Biosciences, San Diego, CA) at a final concentration of 20 nmol·mg<sup>-1</sup> of protein. Proteins were solubilized in 10 mM Tris·HCl (pH 7.4)/150 mM NaCl/10 mM imidazole/1% dodecyl- $\beta$ -D-maltoside (Anatrace, Maumee, OH), and one tablet of Complete protease inhibitors minus EDTA (Roche Diagnostics, Mannheim, Germany) for 1 h at 4°C with stirring. Particulate material was removed by ultracentrifugation at 140,000  $\times$  g at 4°C for 45 min. The supernatant was passed through a nickel-nitrilotriacetic acid Superflow (Qiagen, Valencia, CA) column (flow rate, 0.5 ml·min<sup>-1</sup>). The column was washed with 10 mM Tris·HCl (pH 7.4)/150 mM NaCl/0.05% dodecylmaltoside/5  $\mu$ M ATR, containing first 40 mM and then 60 mM imidazole. The carrier was eluted in the same buffer containing 200 mM imidazole. The eluate was concentrated to 2 mg·ml<sup>-1</sup> in a YM-30 Centricon (Millipore, Billerica, MA) and purified on a Superdex 200 XK16/60 column (GE Healthcare, Little Chalfont, U.K.) in buffer containing 10 mM Tris·HCl (pH 7.4), 150 mM NaCl, 0.05% dodecylmaltoside, and 5  $\mu$ M ATR.

**Reconstitution of Purified AAC2.** Liposomes were prepared by using *E. coli* total lipid extract and egg yolk phosphatidylcholine (Avanti Polar Lipids) in a 3:1 (wt/wt) ratio in 50 mM KPi buffer, pH 7.0, at a final lipid concentration of 20 mg·ml<sup>-1</sup>. Liposomes were passed nine times through a membrane with 1- $\mu$ m pores (Whatman, Clifton, NJ) to make them unilamellar, and they were destabilized with Triton X-100 (*SI Methods*). Purified carrier protein (20  $\mu$ g) and destabilized liposomes (10 mg) were added to 50 mM KPi buffer (pH 7.0), with 0.2% (vol/vol) Triton X-100 and 5 mM ADP (3-ml total volume), and the suspension was mixed. Detergent was removed with Biobeads (240 mg) (Bio-Rad, Hercules, CA) and gentle rotation for 2 h at 4°C. The Biobeads were removed by filtration and the procedure was repeated twice more. The proteoliposomes were collected by centrifugation at 300,000  $\times$  g for 30 min at 4°C. The pellet was resuspended in KPi buffer containing 5 mM ADP to a final volume of 1 ml.

**Transport Assays.** Proteoliposomes or fused membranes were extruded 9 times in the presence of 5 mM ADP through a membrane with 1- $\mu$ m pores (Whatman). When required, 3 mM MTSES (Anatrace) was added before extrusion. The extruded membranes were harvested by centrifugation at 300,000  $\times$  g for 30 min at 4°C. The pellet was resuspended in KPi buffer containing 5 mM ADP. The external ADP was removed on a Sephadex G-75 gel filtration column (3.5-ml bed volume) equilibrated with KPi buffer. The proteoliposomes or fused membranes were eluted in 1 ml of KPi buffer. Transport was initiated by diluting 100  $\mu$ l of membranes in 300  $\mu$ l of KPi buffer containing 1.35  $\mu$ M [8-<sup>14</sup>C]-ADP (Perkin-Elmer, Waltham, MA). The experiments were performed at 12°C with constant stirring. At intervals, the uptake of radio-labeled substrate was quenched by adding ice cold KPi buffer (4 ml), and immediately the mixture was filtered through cellulose nitrate membranes (0.45  $\mu$ m pore size). The filters were washed with ice-cold KPi buffer (2 ml), and incorporated radioactivity was determined by scintillation counting. The initial uptake rates of [<sup>14</sup>C]-ADP were determined in quintuplicate in the first 15 s of linear uptake. The amount of AAC2

